Received 10th January 2011, Accepted 7th April 2011
: 10.1039/ 1 01026

Si Quantum dots (QD's) are offering the possibilities for improving the efficiency and lowering the cost of solar cells. In this paper we study the PV-related critical factors that may affect design of Si QDs solar cell by performing atomistic calculation including many-body interaction. First, we find that the weak absorption in bulk Si is significantly enhanced in Si QDs, specially in small dot size, due to quantum-confinement induced mixing of G-character into the *X*-like conduction band states. We demonstrate that the atomic symmetry of Si QD also plays an important role on its bandgap and absorption spectrum. Second, quantum confinement has a detrimental effect on another PV property – it significantly enhances the exciton binding energy in Si QDs, leading to difficulty in charge separation. We observe universal linear dependence of exciton binding energy excitonic gap for all Si QDs. Knowledge of this universal linear function will be helpful to obtain experimentally the exciton binding energy by just measuring the optical gap without requiring knowledge on dot shape, size, and surface treatment. Third, we evaluate the possibility of resonant charge transport in an array of Si QDs *a* miniband channels created by dot-dot coupling. We show that for such charge transport the Si QDs embedded into a matrix should have tight size tolerances and be very closely spaced. Fourth, we find that the loss of quantum confinement effect induced by dot-dot coupling is negligible – smaller than 70 meV even for two dots at intimate contact.

Zero-dimensional (0D) Quantum-dots (QD's) have been advertised to have two types of advantages over one-dimensional (2D) films or three-dimensional (3D) bulk crystals in the functioning of PV solar cells.[1 3] (i)

current-matched to the solar spectrum, raising conversion efficiencies. (b) Light trapping in an active layer of assembled QDs can be realized more efficiently than in traditional PV due to simple, low temperature cell layer assembly on textured substrates (. ., from nanoparticle inks). (c) Radiation tolerance of 0D QD structures was recently found to be two orders of magnitude higher than that of 2D quantum wells,[4] due to the quantum confinement in all three dimensions. Thus, longer lifetimes of QD PV optoelectronics are expected when used in space applications.

Another class of advantages of QD for solar cells involves (ii) *ffT a a . a a ab a* - *a* . This includes effects such as the existence in QD's of significant electron-hole (excitonic) binding, impeding

where $\{\varepsilon$, $\psi($, σ

The a (or exciton transition energy) E_X[24] is approximately the difference in total energy of a QD occupied by an electro-hole pair having as a dominant configuration an electron in the lowest unoccupied molecular orbital (LUMO) $_0$ and a hole in the highest occupied molecular orbital (HOMO) $_0$ and a QD in the ground state,

$$E_X = E_{1,1}(\tfrac{1}{0}, \tfrac{1}{0}) - E_{0,0}. \quad (8)$$

Here $E_{1,1}(\tfrac{1}{0}, \tfrac{1}{0}) = \varepsilon_{\ _0} - \varepsilon_{\ _0}$

the contribution of space confinement enhanced electron-hole

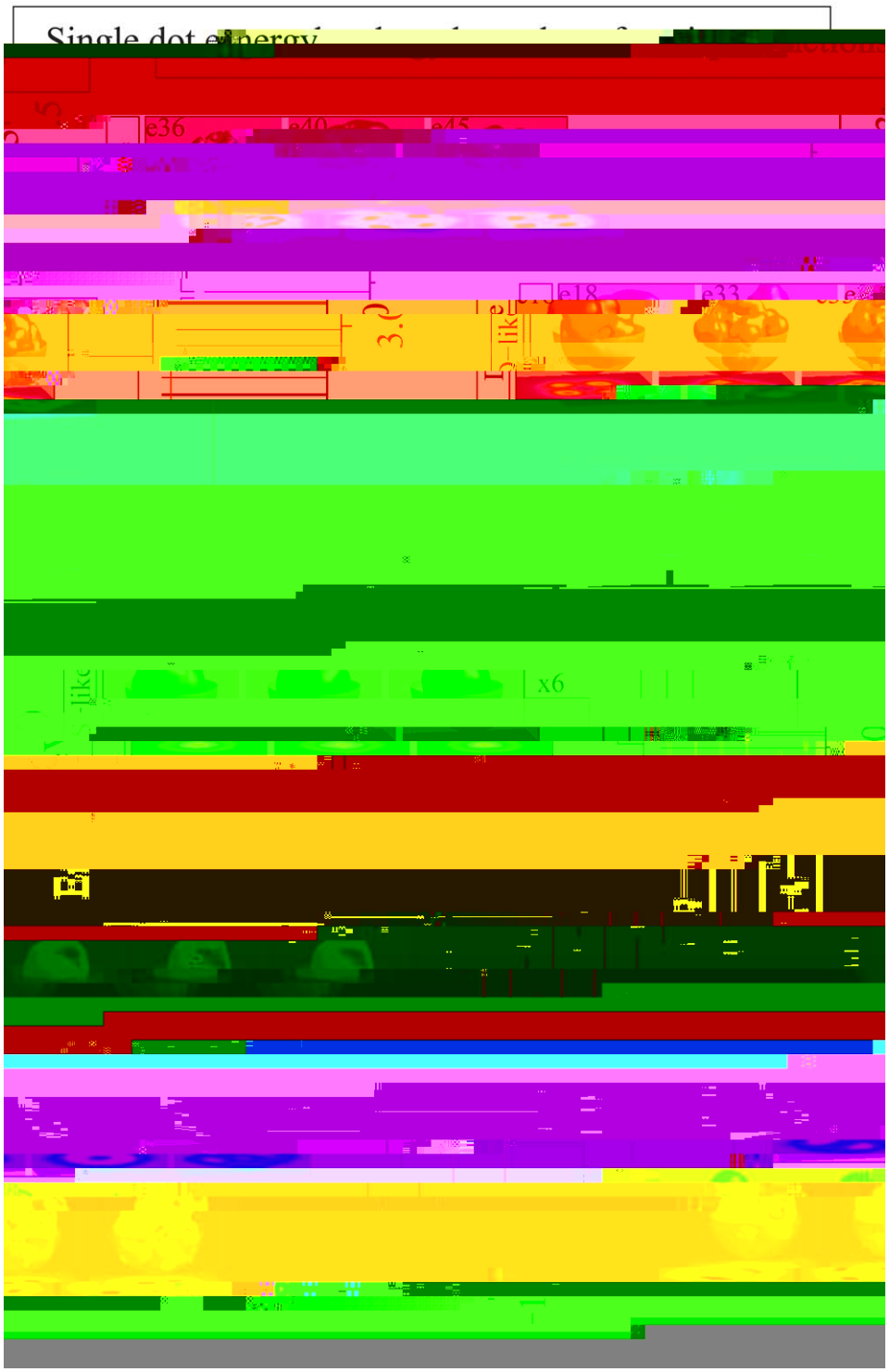

. **6** Left panels show the envelop function ψ ( )

an intimate contact (0 Å) affects the transition energies by only about 50 meV and results in relatively minor widening of the low energy spectral peaks as shown in Fig. 12. This indicates that the quantum confinement is preserved even at intimate proximity, and that level splitting is unlikely to exceed 50–100 meV. We note that in Si QD arrays, the experimental measurements of absorption spectra yield smooth energy-dependency without peaks such as in Fig. 12. Since these measurements are typically performed on either isolated dots in solution or on Si QDs in SiO_2 matrix separated by about 1 nm, we conclude that size, shape, and symmetry-related energy level fluctuations of the current state-of-the-art Si QDs likely exceed 100 meV making

the structure of the spectrum unobservable. This is consistent with Fig. 8 and with Fig. 3 assuming 10% size variation.

The level repulsion E_R (which is related to half the miniband width in an ordered dot array) of LUMO and HOMO is calculated in Fig. 13 for Si dot-dimer embedded in SGM and LGM. It is plotted as function of face-to-face separation in the Si dot-dimer. The results of Fig. 13 (red curve, dimer of two almost identical Si dots) demonstrate that even for zero separations, the level half-splitting (level repulsion E_{R}) due to dot-dot interaction is only about 60 meV. This is comparable with disorder energies introduced by symmetry, shape, and size variations as discussed above. The level splitting exponentially decays with increasing the dot-dot separation. Moreover, the splitting is further reduced, to less than 10 meV, for larger size 4 nm dots dimer (black curve). The observed scatter in the data away from the trends is due to the different atomic symmetry of dots (T_{d} . C_3). Fig. 13 shows that the level splitting and thus, miniband formation, effectively ceases at face-to-face separations greater than 5 Å for low-barrier matrix and already at 2 Å for high barrier matrix. This very sensitive interdot distance dependence can explain very low currents observed in the cell device with Si QDs embedded in SiO_2 matrix.[31] Thus, at least for the matrix with band offsets of 1 eV or greater, it seems unlikely that the dot-dot interaction accompanied by

level splitting is also strongly affected by the size variations of the neighboring dots. This is demonstrated in Fig. 13 by the red, green, and blue curves that correspond to size difference between the two dots of $\Delta R/R = 0$, 10, 20%. Fig. 13 shows that dot size difference of 10 to 20% significantly reduces the level splitting. This size uniformity dependence has strong implications for carrier transport in Si QD systems such as solar cell absorber layers.

The photo-generated electron-hole pairs must be separated into free electron and hole carriers and travel to their respective negative and positive electrodes for the electrical energy to be useful. The poor carrier transport because of the carrier localization inside the dot has to be overcome in the QD solar

nearest hopping sites and separated by distance with energies E

disorder in the energy landscape. Two main mechanisms have been considered to describe carrier transport in semiconductor nanostructures:[42] transport in a miniband and hopping between Wannier-Stark states. In comparison with miniband conduction, the hopping conduction exhibits low carrier mobility μ f $(-)$ $\left(-\frac{E-E}{{}_{B}T}\right)$ associated with two

dependence is not affected by the matrix bandgap. At the PL bandgap of 2 eV that corresponds to 2 nm size dots in 3.2 eV matrix, and about 2.8 nm dots in 5.9 eV matrix, the exciton binding energy is about 200 meV. Such a considerable binding energy resembles that observed in organic semiconductors and is expected to affect the charge separation.[34] We have to note, however, that the exciton binding energies are likely to be lower in dense arrays of Si dots as compared to isolated dots in matrix, due to higher average dielectric constant introduced by the Si dots. At present, however, Si QD volume fractions in experimentally grown films (. . with Si particles embedded into SiO2 matrix) are relatively low. This, along with the negligible dot-dot interaction as supported by data of Fig. 8 and 9 at the surface-surface distances typically found in those films (∼1 nm), might provide a possible explanation of poor carrier collection achieved experimentally so far. Closely-packed Si QD arrays might be necessary to reduce the exciton binding energy. Alternatively, Si QDs in combination with materials/structures that facilitate exciton dissociation (such as Si QD/P3HT hybrid absorber layers,[50] might enable advantages of excitonic effects.

By performing atomistic calculation including many-body interaction we have studied the important PV-related critical

32 S. Takeoka, M. Fujii and S. Hayashi, *P . R . B: C . Ma* , 2000, **62**, 16820.
33 F. Meillaud, A. Shah, C. Droz, E. Vallat-Sauvain and C. Miazza, *S . E Ma . S . C* , 2006, **90**, 2952.
34 B. A. Gregg, *J. P . C . B*, 2003, **107**, 4688.
35 G. D. Scholes and G. Rumbles, *Na . Ma .*, 2006, **5**, 683.
36 F. A. Reboredo, A. Franceschetti and A. Zunger, *P . R . B: C . Ma* , 2000, **61**, 13073.
37 A. Franceschetti, A. Williamson and A. Zunger, *J. P . C . B*, 2000, **104**, 3398.
38 K. Nishiguchi, X. Zhao and S. Odaa, *J. A . P .*, 2002, **92**, 2748.
39 M. Sykora, L. Mangolini, R. D. Schaller, U. Kortshagen, D. Jurbergs and V. I. Klimov, *P . R . L .*, 2008, **100**, 067401.
40 G. M. Dalpian, M. L. Tiago, M. L. del Puerto and J. R. Chelikowsky, *Na L .*, 2006, **6**, 501.
41 S. V. Goupalov, *P . R . B*, 2009, **79**, 23305.
42 H. T. G
73 -299.0429 -16.1238 TD (2000,)Tj /F1 18Tf 2.5607 0 TD (104)Tj /F3 8f .4979 0 TD [(,)-299.1(501.)